



# STABILITY OF THERMALLY DRIVEN SHEAR FLOWS IN LONG INCLINED CAVITIES WITH END-TO-END TEMPERATURE DIFFERENCE

*A.Rohith Roshan<sup>1</sup>, V.V.Divya<sup>2</sup> and K.Sumathi<sup>3</sup>*

<sup>1</sup> Department of Mechanical Engineering, Government College of Technology, Coimbatore 641013

<sup>2</sup> Department of Mathematics with Computer Applications, PSG College of Arts and Science, Coimbatore 641014

<sup>3</sup> Department of Mathematics, PSGR Krishnammal College for Women, Coimbatore 641004

**Abstract:** *In this paper we investigate the stability of buoyancy driven shear flows in inclined long cavities with end wall temperature difference. Analytical expressions are found for the growth rate and stream function as a function of wave number and the stability of the flow is discussed for different inclinations and a wide range of Prandtl number.*

## 1. Introduction

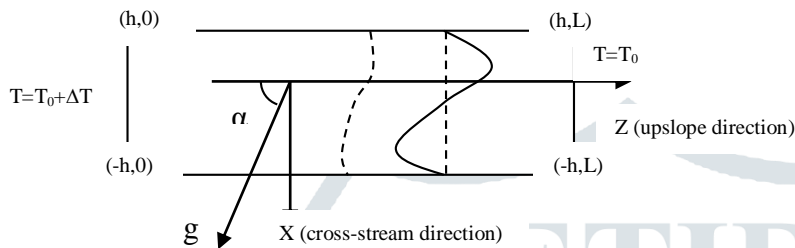
Convection in long inclined cavities driven by a temperature gradient along their longest axis is also important for a variety of phenomena that occur in industry and nature. For instance in crystal growth for vapour phase, larger transport arises. In the literature most of the published works considered cavities placed horizontally (Daniels and Wang(1994)).

In the inclined cavity of shown in the figure, the basic flow arises for any temperature difference and its intensity increases steeply with Rayleigh number as long as the isotherms are distorted by advection. The type of flow that arises is similar to that described by Woods and Linz [1992] in inclined liquid –filled rock fractures with vertical thermal gradient. Delgado –Buscalioni and Crespo del Arco (1999) studied the basic and secondary flow in an inclined cavity filled with an incompressible viscous fluid. A classical review of earlier works can be seen in the papers by Hart (1971, 1981, 2000).

In this work we study the stability of buoyancy driven shear flows in inclined long cavities with end wall temperature difference. Using regular perturbation method, approximations of flow characteristics are found and effect of various nondimensional numbers are discussed numerically with the help of graphs.

## 2. Flow Description

We consider the flow in the two dimensional thermally driven shear flow in axially heated inclined long cavities. The cavity is filled with an incompressible viscous fluid and inclined  $\alpha$  degrees with respect to gravity. We have employed Boussinesq approximation and assume that a convective motion is established due to a temperature difference between the end walls. That is, it is assumed that in the inclined cavity under consideration, the basic flow arises for any temperature difference and its intensity increases steeply with the Rayleigh number as long as the isotherms are distorted by advection. The geometry of the problem and the structure of the basic flow are shown below.



Shear flow in long inclined cavities with end to end temperature difference

The equations governing the motion are given below

$$\nabla^* \vec{q}^* = 0 \tag{1}$$

$$\rho \left[ \frac{\partial \vec{q}^*}{\partial t^*} + (\vec{q}^* \cdot \nabla^*) \vec{q}^* \right] = -\nabla P^* - \rho^* \vec{g}^* \hat{e}_g + \mu \nabla^2 \vec{q}^* \tag{2}$$

$$\frac{\partial T^*}{\partial t^*} + (\vec{q}^* \cdot \nabla^*) T^* = k \nabla^2 T^* \tag{3}$$

$$\rho^* = \rho_0 (1 - \beta_p^* (T^* - T_0)) \tag{4}$$

Introducing  $h^2/\gamma$ ,  $h, \gamma/h$  and  $\Delta T h/L$  as scales for time, length, velocity and temperature respectively in equations (1) to (4), we get the nondimensional equations as follows.

$$\nabla \cdot \vec{v} = 0 \tag{5}$$

$$\frac{\partial \vec{v}}{\partial t} + (\vec{v} \cdot \nabla) \vec{v} = -\nabla p + \Delta \vec{v} - RPr^{-1} T e_g \tag{6}$$

$$\frac{\partial T}{\partial t} + (\vec{v} \cdot \nabla) T = Pr^{-1} \Delta T \tag{7}$$

where

$$\vec{e}_g = \sin \alpha \hat{i} - \cos \alpha \hat{k}, \text{ is the gravity vector.}$$

Subject to boundary conditions

$$\vec{v} = \vec{0}$$

$$\frac{\partial T}{\partial t} = 0 \text{ at } x = \pm 1 \tag{8}$$

Equilibrium velocity and temperature profiles are assumed to be

$$\vec{q}_e = (u_o, 0, w_o) \text{ and} \tag{9}$$

$$T_o = -\eta z + b + \theta_o(x) \tag{10}$$

The equilibrium velocity and temperature are given by

$$w_o(x) = \frac{r \tan \alpha}{Pr} \left( \frac{\sin r \sinh rx - \sinh r \sin rx}{d(r)} \right) \tag{11}$$

$$\theta_o(x) = -\eta \frac{\tan \alpha}{r} \left( \frac{\sin r \sinh rx + \sinh r \sin rx}{d(r)} - rx \right) \tag{12}$$

where

$$d(r) = \sinh r \cos r + \cosh r \sin r \tag{13}$$

and

$$r = (\eta R \cos \alpha)^{1/4} \tag{14}$$

In order to study the stability of the basic flow, the flow variables are written as the sum of the mean flow quantity and a small perturbation.

The stream function of the perturbation flow satisfies  $u = \frac{\partial \psi}{\partial z}$ ,  $w = -\frac{\partial \psi}{\partial x}$ .

We ascribe to the stream function and temperature perturbation

$$\lambda \left( \frac{d^2}{dx^2} - k^2 \right) \varphi = \left( \frac{d^2}{dx^2} - k^2 \right)^2 \varphi - ik \left( w_o \left( \frac{\partial^2}{\partial x^2} - k^2 \right) \varphi - w_o''(\varphi) \right) - RP_r^{-1} (ik \sin \alpha \theta + \cos \alpha \theta') \tag{15}$$

$$\lambda \theta = P_r^{-1} \left( \frac{d^2}{dx^2} - k^2 \right) \theta - ik (\theta_o' \varphi + w_o \theta) - \psi' \tag{16}$$

$$\text{Boundary conditions are } \varphi(\pm 1) = \varphi'(\pm 1) = 0, \quad \theta'(\pm 1) = 0 \tag{17}$$

### 3 Analysis

In this section we analyze the behavior of the disturbances for long waves i.e., k is assumed to be small. We attempt to find analytical expressions for the growth rate and stream using regular perturbation method.

Assuming

$$\lambda = \lambda_o + k^2 \lambda_1 + \dots$$

$$\theta = T_o + kT_1 + k^2T_2 + \dots$$

$$\varphi = \varphi_o + k \varphi_1 + k^2 \varphi_2 + \dots \tag{18}$$

And substituting in (15) – (18) and solving we get

$$\varphi_o = \cosh(x) + A_1 \cosh(R_2x)$$

$$T_o = A_2 \cosh(\sqrt{\lambda_o Pr}x) + A_3 \sinh(\sqrt{\lambda_o Pr}x) + \frac{R_1}{P_r^{-1}R_1^2 - \lambda_o} \sinh(R_1x) +$$

$$\frac{R_2 A_1}{P_r^{-1}R_2^2 - \lambda_o} \sinh(R_2x)$$

Applying the boundary conditions we get the eigenvalues and eigen functions as follows.

$$R_2 \sinh (R_1) \cosh (R_2) - R_1 \sinh (R_2) \cosh (R_1) = 0$$

$$R_2 \cosh (R_1) \sinh (R_2) - R_1 \cosh (R_2) \sinh (R_1) = 0$$

The above expressions do not give explicit values for  $\lambda_0$ . Hence the values of  $\lambda_0$  are obtained using the software Mathematica 8.0.

$$\begin{aligned} \varphi_1 = & A_5 \cosh (R_1 x) + A_6 \sinh (R_1 x) + A_7 \cosh (R_2 x) + A_8 \sinh (R_2 x) \\ & + A_9 \lambda_1 \cosh (\sqrt{\lambda_0 P_r} x) \\ & + A_{10} \lambda_1 x \sinh (R_1 x) \\ & + A_{11} \lambda_1 x \sinh (R_2 x) \\ & + A_{12} x \cosh (R_1 x) + A_{13} x \cosh (R_2 x) \\ & + A_{14} \sinh ((r+R_1) x) + A_{15} \sinh ((r-R_1) x) \\ & + A_{16} \sinh ((r+R_2) x) + A_{17} \sinh ((r-R_2) x) \\ & + A_{18} \sin ((r+i R_1) x) + A_{19} \sin ((r-i R_1) x) \\ & + A_{20} \sinh ((r+i R_2) x) + A_{21} \sinh ((r-i R_2) x) \\ & + A_{22} \sinh ((r+\sqrt{\lambda_0 P_r}) x) + A_{23} \sinh ((r-\sqrt{\lambda_0 P_r}) x) \\ & + A_{24} \sinh ((r-i \sqrt{\lambda_0 P_r}) x) + A_{25} \sinh ((r+i \sqrt{\lambda_0 P_r}) x) \end{aligned}$$

For brevity, the constants are given in *Appendix*.

#### 4. Results and Discussion

We consider the flow in the two dimensional thermally driven shear flow in axially heated inclined long cavities. The cavity is filled with an incompressible viscous fluid and inclined  $\alpha$  degrees with respect to gravity. We have employed Boussinesq approximation and assume that a convective motion is established due to a temperature difference between the end walls. The effect of inclined boundaries on the stability of the basic flow in axially heated long inclined cavity is the main concern of this work. Hence we have found the value of the growth rate as a function of Prandtl number, Rayleigh number and angle of inclination numerically and plotted them in figures (1) –(6).

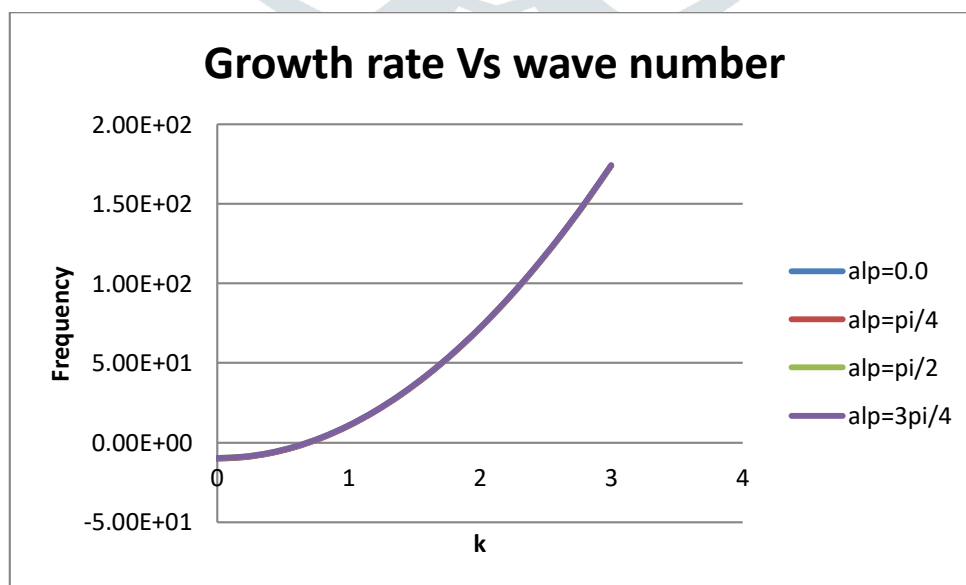


Figure 1 Growth rate as a function of wave number (Pr =0.7, R=10.0)

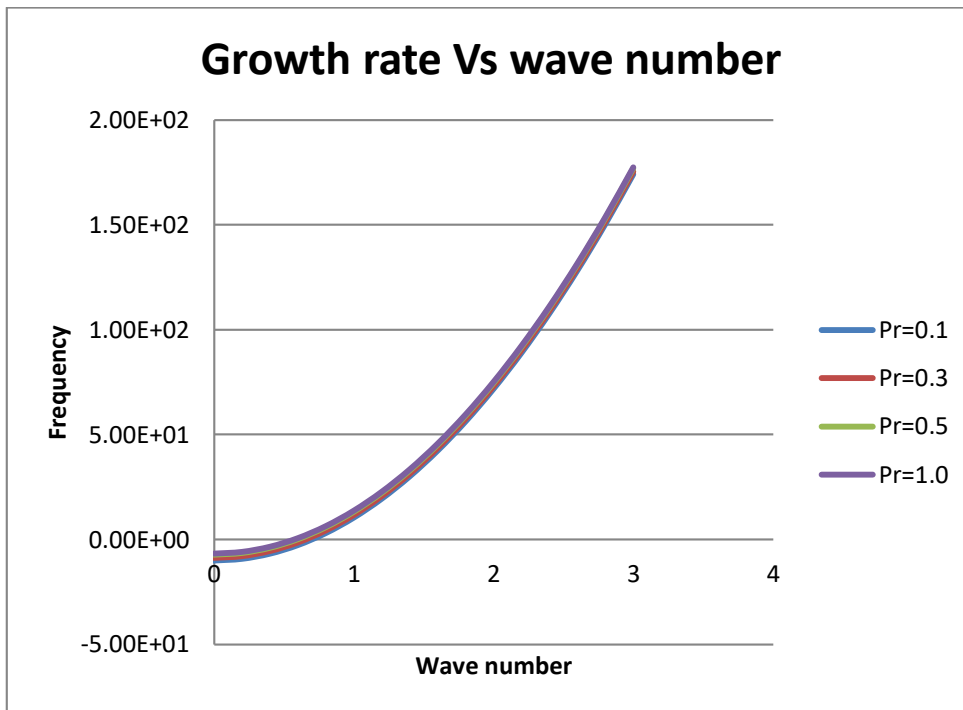


Figure 2 Growth rate as a function of wave number ( $\alpha = \pi/3.0, R=10.0$ )

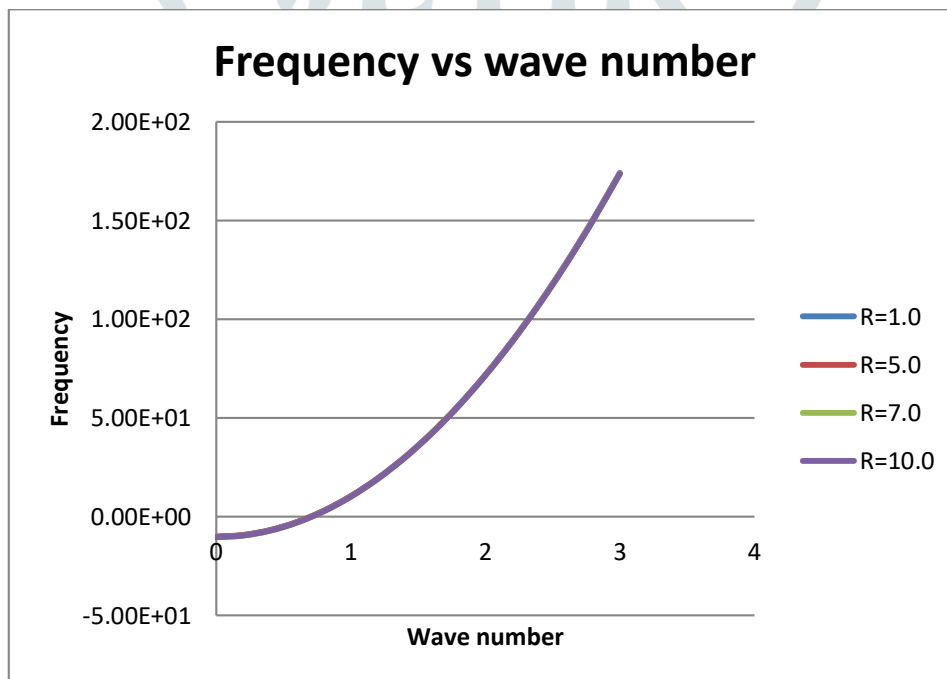


Figure 3 Growth rate as a function of wave number ( $\alpha = \pi/6.0, Pr=0.7$ )

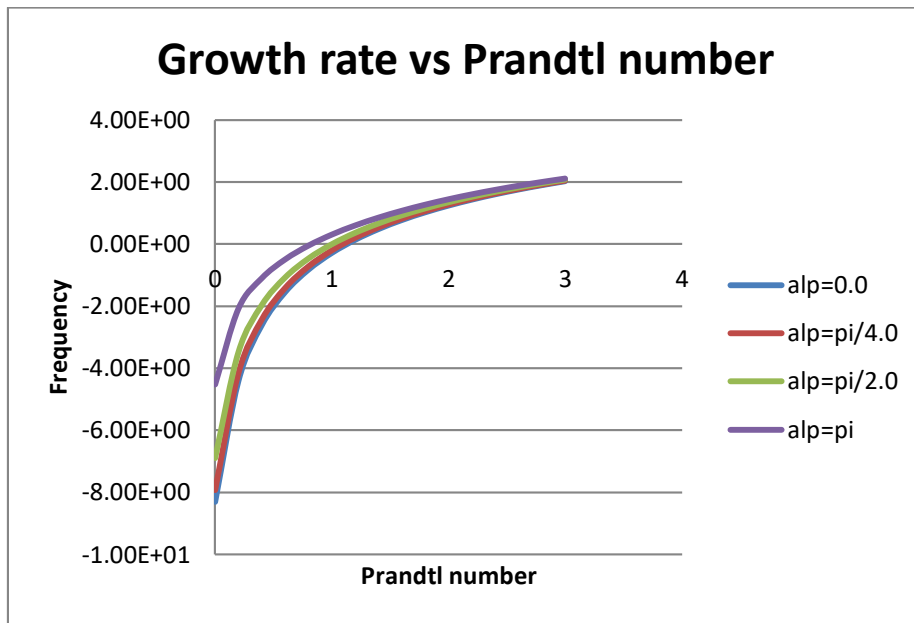


Figure 4 Growth rate variation with respect to Prandtl number ( $\alpha = \pi/6.0, R=10.0$ )

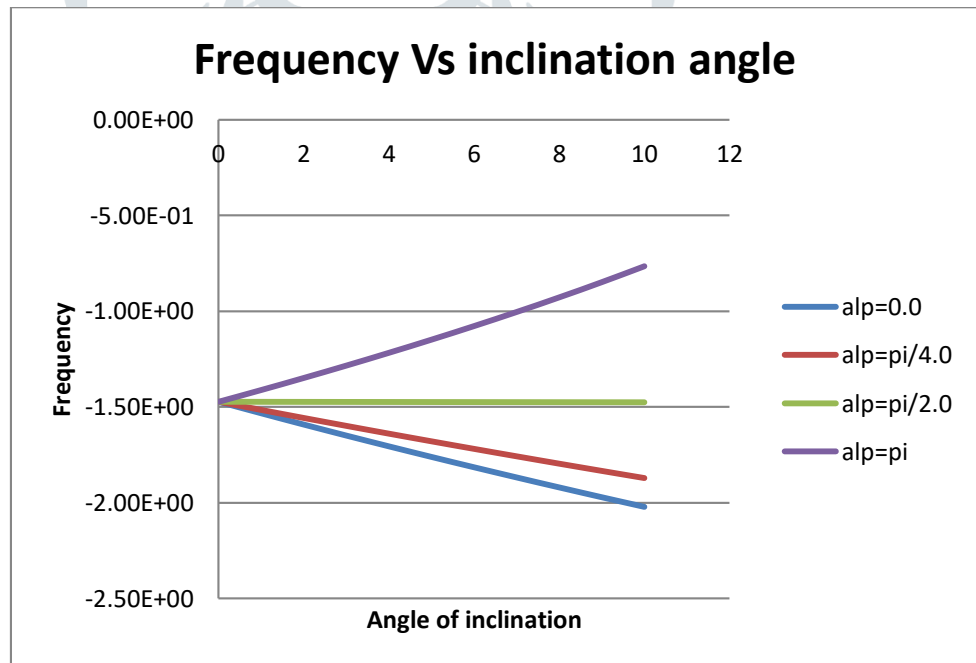


Figure 5 Growth rate variation with respect to Angle of inclination ( $Pr=0.7, R=10.0$ )

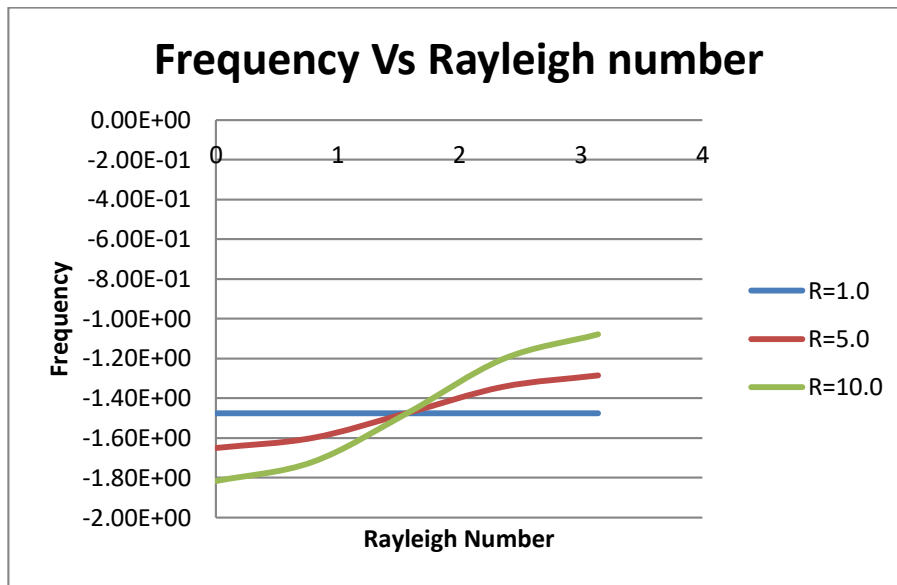


Figure 6 Growth rate variation with respect to R (Pr=0.7,alpha=pi/3)

It was found from these figures that Rayleigh number plays a significant role in enhancing the stability of the flow. We can see that the real part of the growth rate decreases due to increase in Rayleigh number. Angle of inclination and Prandtl number is found to increase the growth rate.

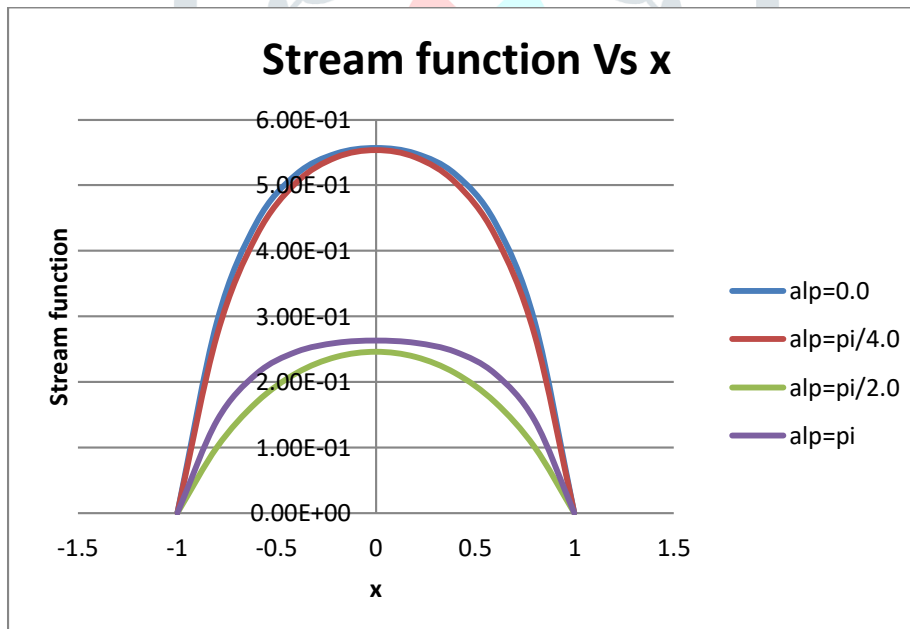


Figure7 Stream function variation wrt x (Pr=0.7,R=10.0)

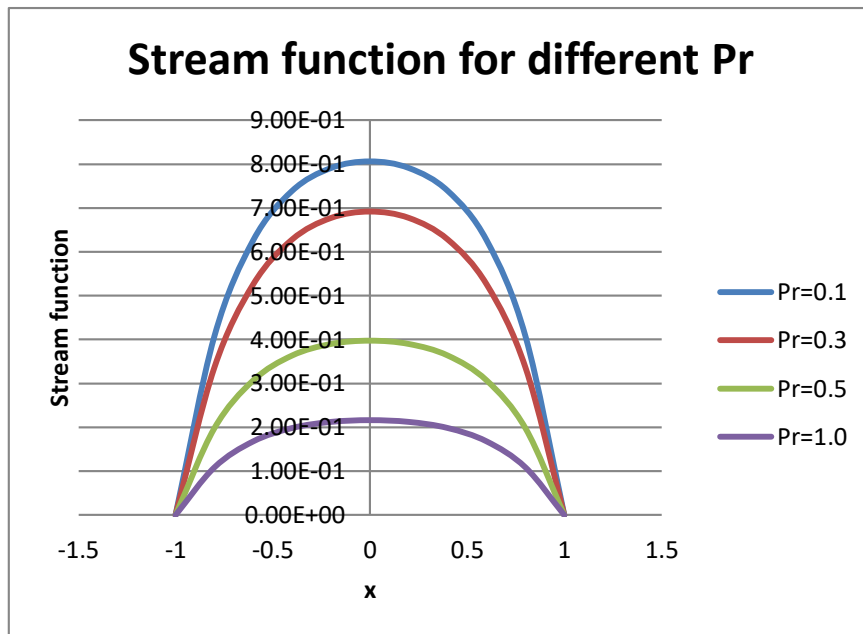


Figure 8 Stream function variation wrt x ( $\alpha = \pi/3, R = 10.0$ )

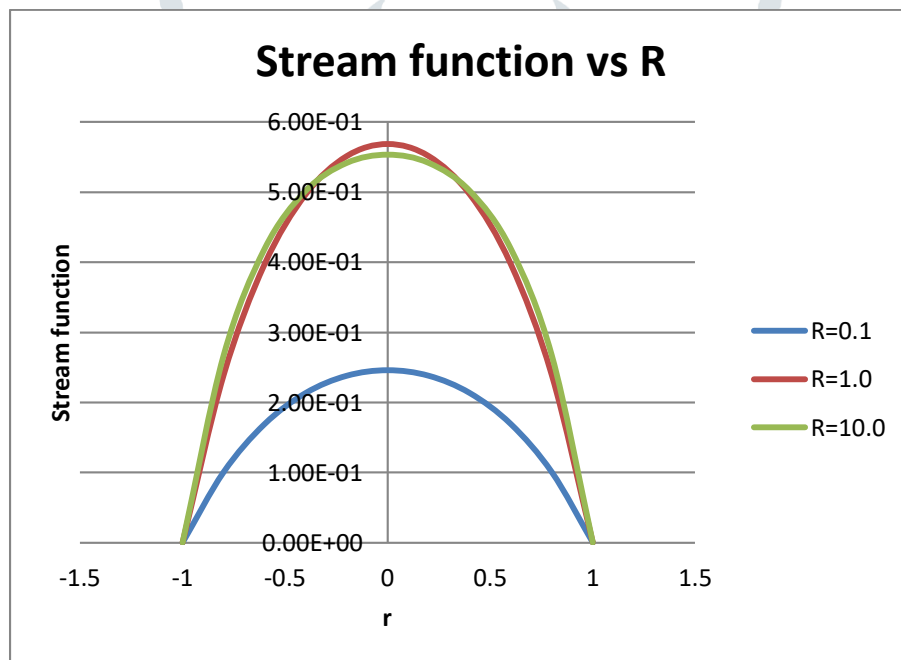


Figure 9 Stream function variation wrt x ( $\alpha = \pi/3, Pr = 0.7$ )

Figures (7) – (9) show that increase in angle of inclination, Prandtl number and the wave number are found to decrease the stream function of the disturbances. Hence we can infer that by increasing the angle of inclination we can stabilize the flow.



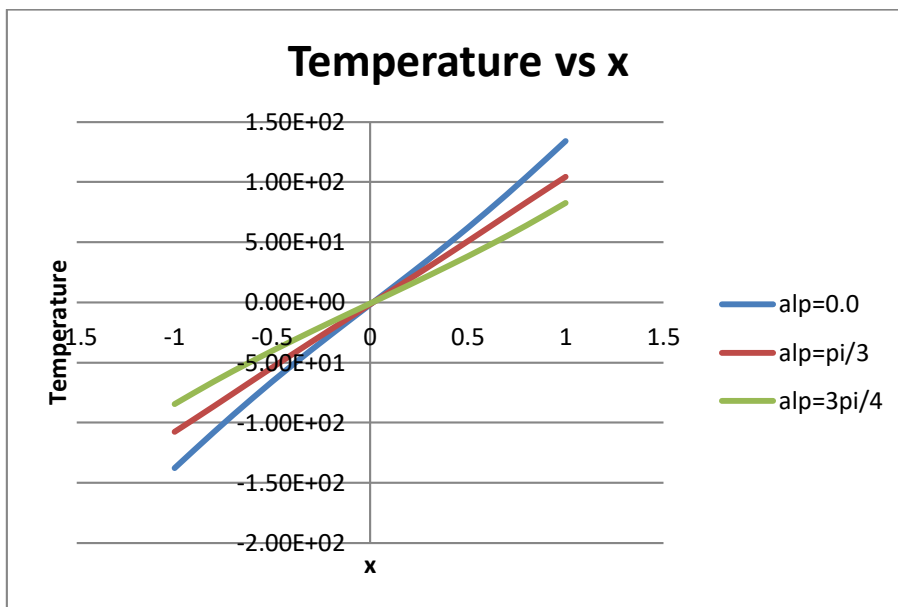


Figure 10 Temperature distribution as a function of  $x$  ( $k=0.5, Pr=0.7, R=10.0$ )

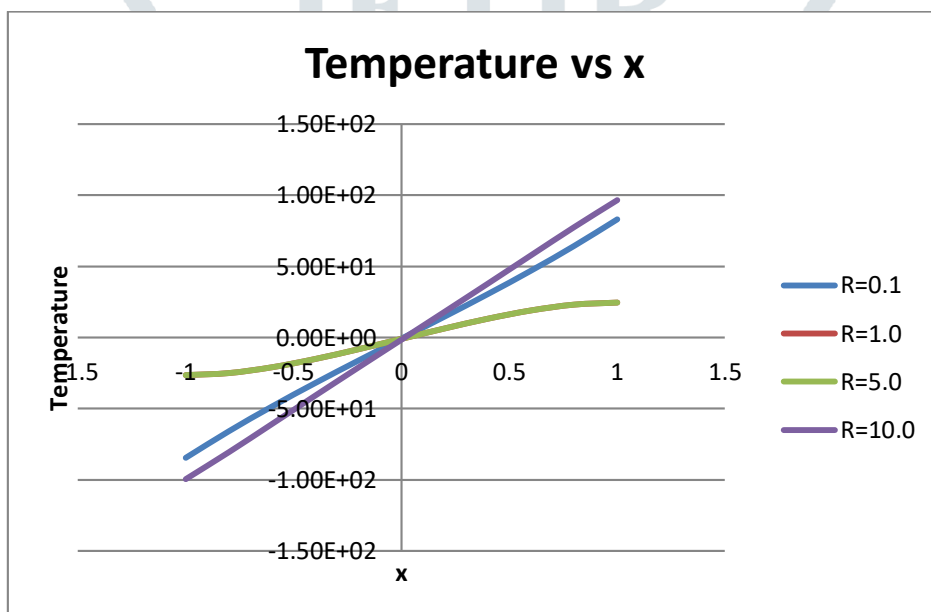


Figure 11 Temperature distribution as a function of  $x$  ( $k=0.5, Pr=0.7, \alpha = \pi/6$ )

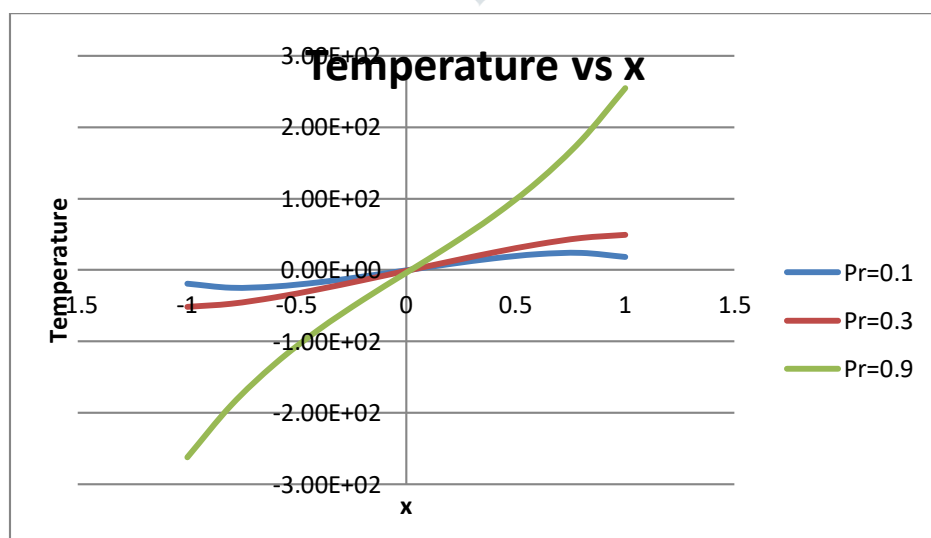


Figure 12 Temperature distribution as a function of  $x$  ( $k=0.5, R=10.0, \alpha = \pi/6$ )

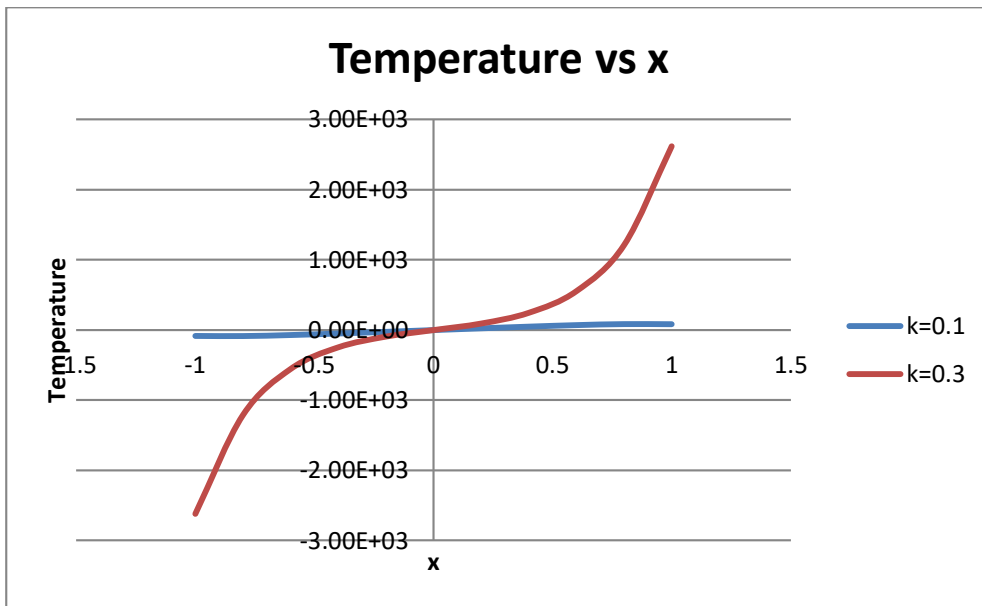


Figure 13 Temperature distribution as a function of  $x$  ( $Pr=0.7, R=10.0, \alpha = \pi/6$ )

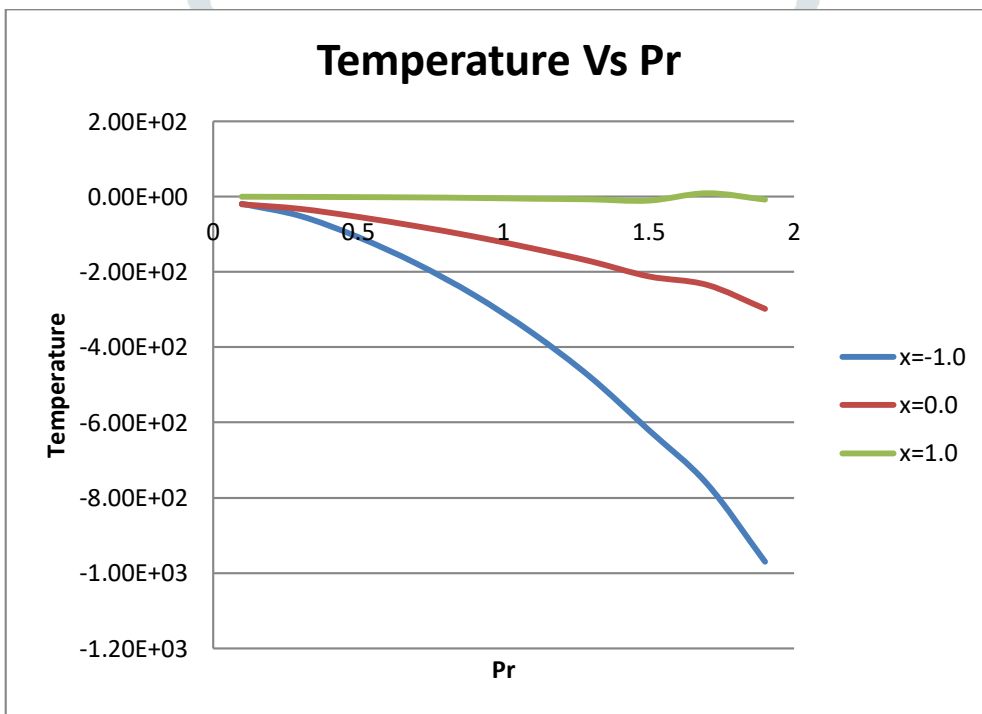


Figure 14 Temperature distribution as a function of  $Pr$  ( $k=0.4, R=10.0, \alpha = \pi/6$ )

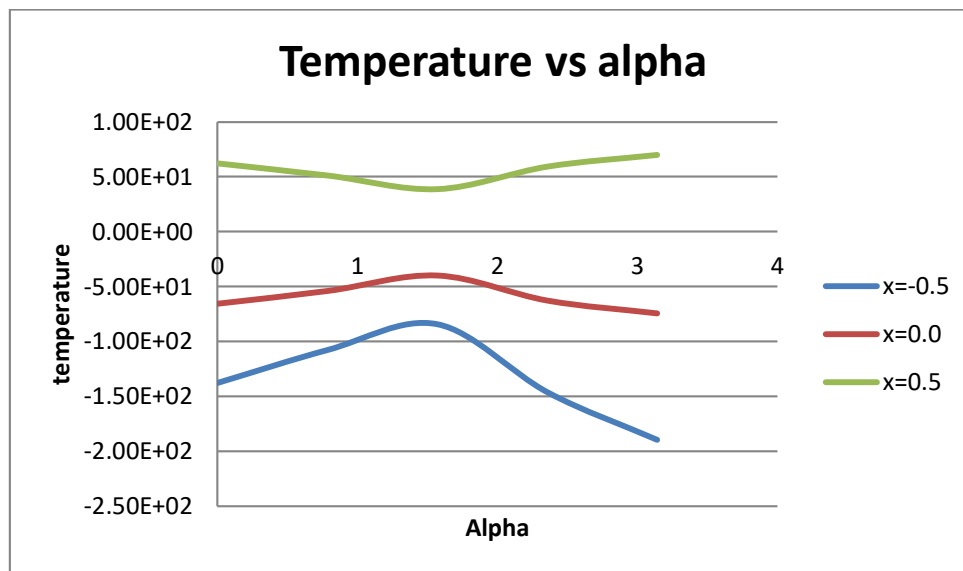


Figure 15 Temperature distribution as a function of  $\alpha$  ( $k=0.4, R=10.0, Pr=0.71$ )

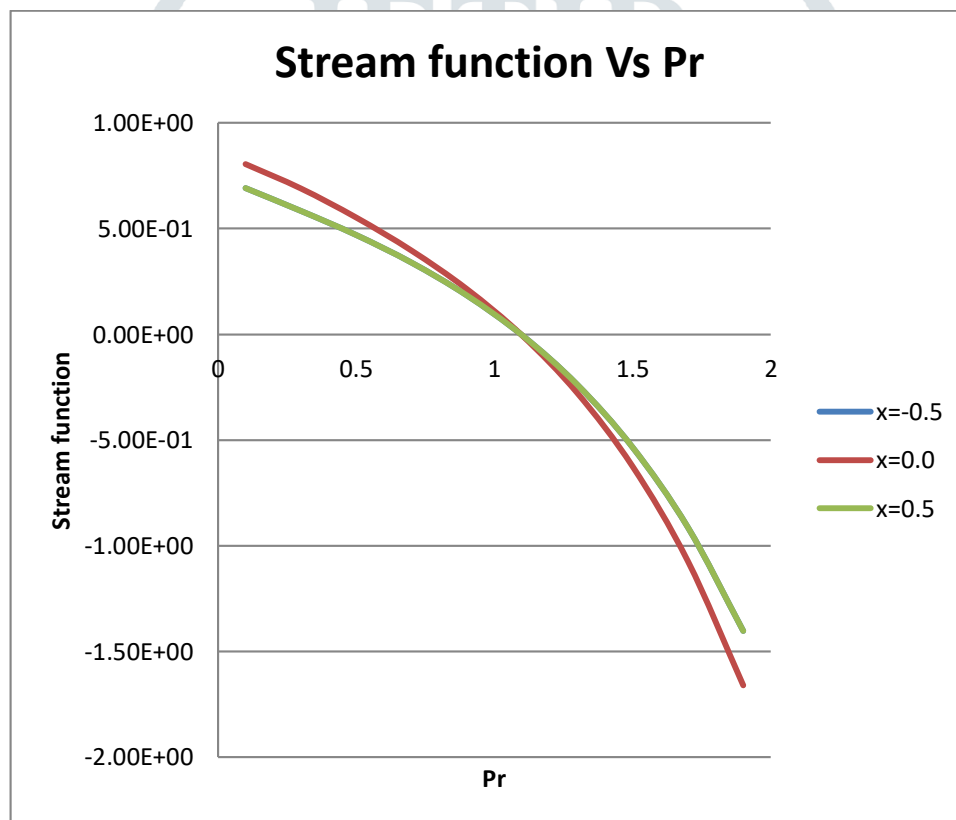


Figure 16 Stream function as a function of  $Pr$  ( $k=0.4, R=10.0, \alpha=\pi/6.0$ )

From Figures (10) – (16) it can be seen that temperature profile increases with the increase in the Rayleigh number, Prandtl number and wave number. Increase in the angle of inclination of the cavity decreases the temperature of the flow.

## 5. Conclusions

In this work we investigated the stability of buoyancy driven shear flows in inclined long cavities with end wall temperature difference. Analytical expressions are found for the growth rate and stream as a function of wave number and the stability of the flow is discussed for different inclinations and a wide range of Prandtl number.

Some of the important findings are

- Rayleigh number plays a significant role in enhancing the stability of the flow. Real part of the growth rate decreases due to increase in Rayleigh number.
- Angle of inclination and Prandtl number are found to increase the growth rate.
- Increase in angle of inclination, Prandtl number and the wave number are found to decrease the stream function
- Temperature profile increases with the increase in the Rayleigh number, Prandtl number and wave number.
- Increase in the angle of inclination of the cavity decreases the temperature of the flow.

### References

1. **Buscalioni, R.D. and Crespo del Arco, E.,** ‘The stability of thermally driven shear flows in long inclined cavities with end to end temperature difference, *Int. J. Heat and mass Transf.*, **42**, 2811 (1999)
2. **Daniels, P.G and Wang, P.** ‘On the evolution of thermally driven shallow cavity flows’ *J. Fluid Mech.*, **259**, 107 (1994)
3. **Hart, J.E.,** ‘Stability of the flow in a differentially heated inclined box’, *J. Fluid Mech.*, **47**, 547 (1971)
4. **Hart, J.E.,** ‘Wave number selection in nonlinear baroclinic instability’ *J. Atmos. Sci.*, **38**, 400 (1981)
5. **Hart J.K,** ‘ The modulation of convection by a lateral shear’, *J. Atmos. Sci.*, **57**, 1169 (2000)
6. **Wood, A.W. and Lintz., S.J,** ‘Natural convection and dispersion in a tilted fracture’ *J. Fluid Mech.*, **241**, 59 (1992)

### Appendix

$$\begin{aligned}
 r &= (\eta R \cos \alpha)^{\frac{1}{4}} \\
 dr &= \sinh r \cos r + \cosh r \sin r \\
 C_1 &= \frac{r \tan \alpha \sin r}{Pr \frac{dr}{dr}} \\
 C_2 &= -\frac{r \tan \alpha \sinh r}{Pr \frac{dr}{dr}} \\
 C_3 &= -\frac{r \frac{dr}{dr}}{\eta \tan \alpha \sin r} \\
 C_4 &= -\frac{r \frac{dr}{dr}}{\eta \tan \alpha \sinh r} \\
 C_5 &= \eta \tan \alpha \\
 w_0 &= C_1 \sinh(rx) + C_2 \sin(rx) \\
 \theta_0 &= C_3 \sinh(rx) + C_4 \sin(rx) + C_5 x \\
 R_1 &= \left[ \frac{\lambda_0(1+Pr) + \sqrt{\lambda_0^2(1-Pr)^2 + 4R \cos \alpha}}{2} \right]^{\frac{1}{2}} \\
 R_2 &= \left[ \frac{\lambda_0(1+Pr) + \sqrt{\lambda_0^2(1-Pr)^2 + 4R \cos \alpha}}{2} \right]^{\frac{1}{2}} \\
 A_1 &= -\frac{\cosh(R_1)}{\cosh(R_2)} \\
 \varphi_0(x) &= \cosh(R_1 x) + A_1 \cosh(R_2 x) \\
 C_8 &= \frac{R_1}{Pr^{-1} R_1^2 - \lambda_0} \\
 C_9 &= \frac{R_2}{Pr^{-1} R_2^2 - \lambda_0} A_1 \\
 C_{9a} &= -\frac{1}{\sqrt{Pr \lambda_0} \cosh(\sqrt{Pr \lambda_0})} \\
 A_2 &= C_{9a} (C_8 R_1 \cosh(R_1) + C_9 R_2 \cosh(R_2)) \\
 t_0 &= A_2 \sinh(\sqrt{Pr \lambda_0} x) + A_3 \sinh(R_1 x) + A_4 \sinh(R_2 x) \\
 C_{10} &= C_1 (R_1^2 - r^2) \\
 C_{11} &= C_2 (R_1^2 + R_2^2) \\
 C_{12} &= A_1 C_1 (R_1^2 - r^2) \\
 C_{13} &= A_1 C_2 (R_1^2 + r^2) \\
 C_{20} &= C_3 \\
 C_{21} &= C_4 \\
 C_{22} &= C_{18} \left( \frac{R_1^2 - r^2}{2} \right) [(r + R_1)^2 - \lambda_0]
 \end{aligned}$$

$$\begin{aligned}
 C_{23} &= C_{18} \left( \frac{R_1^2 - r^2}{2} \right) [(r - R_1)^2 - \lambda_0] \\
 C_{24} &= C_{18} A_1 \left( \frac{R_2^2 - r^2}{2} \right) [(r + R_2)^2 - \lambda_0] \\
 C_{25} &= C_{18} A_1 \left( \frac{R_2^2 - r^2}{2} \right) [(r - R_2)^2 - \lambda_0] \\
 C_{26} &= C_{19} \left( \frac{R_1^2 + r^2}{2} \right) [(r + iR_1)^2 - \lambda_0] \\
 C_{27} &= C_{19} \left( \frac{R_1^2 + r^2}{2} \right) [(r - iR_1)^2 - \lambda_0] \\
 C_{28} &= C_{19} A_1 \left( \frac{R_2^2 + r^2}{2} \right) [(r + iR_1)^2 - \lambda_0] \\
 C_{29} &= C_{19} A_1 \left( \frac{R_2^2 + r^2}{2} \right) [(r - iR_1)^2 - \lambda_0] \\
 C_{30} &= iRPr^{-1} R_1 \sin \alpha \\
 C_{31} &= iRPr^{-1} A_1 R_2 \sin \alpha \\
 C_{32} &= \frac{C_{20} r}{2} (r + R_1) iRPr^{-1} \cos \alpha \\
 C_{33} &= \frac{C_{20} r}{2} (r - R_1) iRPr^{-1} \cos \alpha \\
 C_{34} &= \frac{C_{21} r}{2} (r + iR_1) iRPr^{-1} \cos \alpha \\
 C_{35} &= \frac{C_{21} r}{2} (r - iR_1) iRPr^{-1} \cos \alpha \\
 C_{36} &= \frac{C_{20} r A_1}{2} (r + R_2) iRPr^{-1} \cos \alpha \\
 C_{37} &= \frac{C_{20} r A_1}{2} (r - R_2) iRPr^{-1} \cos \alpha \\
 C_{38} &= \frac{C_{21} r A_1}{2} (r + iR_2) iRPr^{-1} \cos \alpha \\
 C_{39} &= \frac{C_{21} r A_1}{2} (r - iR_2) iRPr^{-1} \cos \alpha \\
 C_{40} &= \frac{C_{18} A_2}{2} (r + \sqrt{Pr\lambda_0}) iRPr^{-1} \cos \alpha \\
 C_{41} &= -\frac{C_{18} A_2}{2} (r - \sqrt{Pr\lambda_0}) iRPr^{-1} \cos \alpha \\
 C_{42} &= \frac{C_{19} A_2 i}{2} (r - i\sqrt{Pr\lambda_0}) iRPr^{-1} \cos \alpha \\
 C_{43} &= -\frac{C_{19} A_2 i}{2} (r + i\sqrt{Pr\lambda_0}) iRPr^{-1} \cos \alpha \\
 C_{44} &= \frac{C_{18} A_3}{2} (r + R_1) iRPr^{-1} \cos \alpha \\
 C_{45} &= -\frac{C_{18} A_3}{2} (r - R_1) iRPr^{-1} \cos \alpha \\
 C_{46} &= \frac{C_{19} A_3 i}{2} (r - iR_1) iRPr^{-1} \cos \alpha \\
 C_{47} &= -\frac{C_{19} A_3 i}{2} (r + iR_1) iRPr^{-1} \cos \alpha \\
 C_{48} &= \frac{C_{18} A_4}{2} (r + R_2) iRPr^{-1} \cos \alpha \\
 C_{49} &= -\frac{C_{18} A_4}{2} (r - R_2) iRPr^{-1} \cos \alpha \\
 C_{50} &= \frac{C_{19} A_4 i}{2} (r - iR_2) iRPr^{-1} \cos \alpha \\
 C_{51} &= -\frac{C_{19} A_4 i}{2} (r + iR_2) iRPr^{-1} \cos \alpha \\
 A_{12} &= \frac{1}{R_1^2 (R_2^2 - R_1^2)} (C_{30} + \eta \tan \alpha R_1) \\
 A_{13} &= \frac{1}{R_2^2 (R_1^2 - R_2^2)} (C_{31} + \eta \tan \alpha R_2 A_1) \\
 A_{14} &= \frac{1}{(r + R_1)^2 ((r + R_1)^2 - R_1^2) ((r + R_1)^2 - R_2^2)} \\
 A_{15} &= \frac{1}{(r - R_1)^2 ((r - R_1)^2 - R_1^2) ((r - R_1)^2 - R_2^2)} \\
 A_{16} &= \frac{1}{(r + R_2)^2 ((r + R_2)^2 - R_1^2) ((r + R_2)^2 - R_2^2)} \\
 A_{17} &= \frac{1}{(r - R_2)^2 ((r - R_2)^2 - R_1^2) ((r - R_2)^2 - R_2^2)} \\
 A_{18} &= \frac{1}{(r + iR_1)^2 ((r + iR_1)^2 - R_1^2) ((r + iR_1)^2 - R_2^2)} \\
 A_{19} &= \frac{1}{(r - iR_1)^2 ((r - iR_1)^2 - R_1^2) ((r - iR_1)^2 - R_2^2)} \\
 A_{20} &= \frac{1}{(r + iR_2)^2 ((r + iR_2)^2 + R_1^2) ((r + iR_2)^2 + R_2^2)} \\
 A_{21} &= \frac{1}{(r + iR_2)^2 ((r - iR_2)^2 + R_1^2) ((r - iR_2)^2 + R_2^2)}
 \end{aligned}$$

$$\begin{aligned}
 A_{22} &= \frac{-1}{(r+\sqrt{Pr\lambda_0})^2((r+\sqrt{Pr\lambda_0})^2+R_1^2)((r+\sqrt{Pr\lambda_0})^2+R_2^2)} \\
 A_{23} &= \frac{-1}{(r-\sqrt{Pr\lambda_0})^2((r+\sqrt{Pr\lambda_0})^2+R_1^2)((r+\sqrt{Pr\lambda_0})^2+R_2^2)} & A_{24} &= \\
 & \frac{-1}{(r-i\sqrt{Pr\lambda_0})^2((r+i\sqrt{Pr\lambda_0})^2+R_1^2)((r+i\sqrt{Pr\lambda_0})^2+R_2^2)} & A_{25} &= \\
 & \frac{-1}{(r-i\sqrt{Pr\lambda_0})^2((r+i\sqrt{Pr\lambda_0})^2-R_1^2)((r+i\sqrt{Pr\lambda_0})^2-R_2^2)} \\
 C_{52} &= -A_{12} \cosh(R_1) - A_{13} \cosh(R_2) - A_{14} \sinh(r + R_1) - A_{15} \sinh(r - R_1) \\
 & \quad - A_{16} \sinh(r + R_2) - A_{17} \sinh(r - R_2) - A_{18} \sin(r + iR_1) \\
 & \quad - A_{19} \sin(r - iR_1) - A_{20} \sin(r + iR_2) - A_{21} \sin(r - iR_2) \\
 & \quad - A_{22} \sinh(r + \sqrt{Pr\lambda_0}) - A_{23} \sinh(r - \sqrt{Pr\lambda_0}) \\
 & \quad - A_{24} \sin(r - i\sqrt{Pr\lambda_0}) - A_{25} \sin(r + i\sqrt{Pr\lambda_0}) & C_{53} &= -A_{12} \sinh(R_1) - A_{12} \cosh(R_1) - A_{13} R_2 \sinh(R_2) - \\
 & \quad - A_{14}(r + R_1) \cosh(r + R_1) - A_{15}(r - R_1) \cosh(r - R_1).
 \end{aligned}$$

